Hydrogen, Fuel Cell & Energy Storage 10 (2023) 51-67

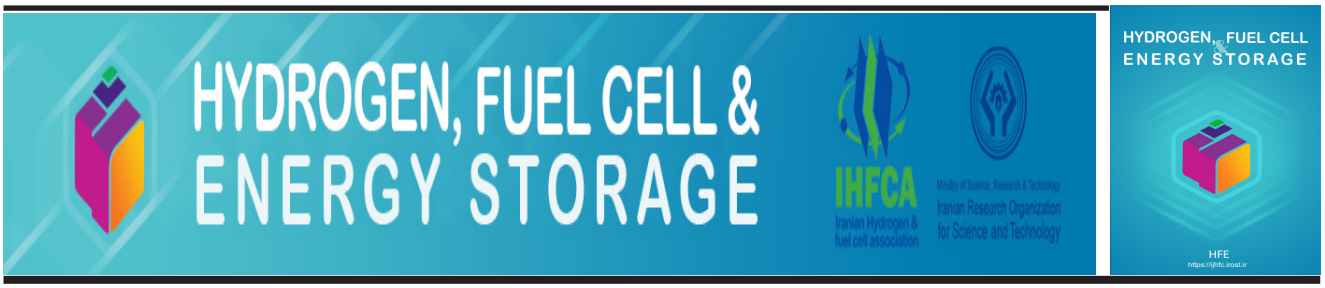

Thermodynamic evaluation of a novel geothermal and solar-driven multigeneration system for hydrogen and freshwater production

Amin Habibzadeh[a], Majid Abbasalizadeh[a, *], Iraj Mirzaee[a], Samad Jafarmadar[a], Hassan Shirvani[b]

[a] Mechanical Engineering Department, Faculty of Engineering, Urmia University, Urmia, Iran
[b] Faculty of Science and Engineering, Anglia Ruskin University, Chelmsford, UK

Article Information

Article History:

Received:
24 Sep 2022
Received in revised form:
10 Oct 2022
Accepted:
11 Oct 2022

Keywords

Energy and exergy analysis
PTC
geothermal
PEM electrolyzer
hydrogen production

Abstract

In this study, a novel multigeneration cycle for hydrogen and freshwater production, including PTC and geothermal as the primary energy sources and Kalina and ORC cycles as the main power production cycles, has been proposed and analyzed from an energy and exergy point of view. The effect of important parameters, including solar irradiation, collector inlet temperature, collector volumetric flow, environment temperature, and geothermal temperature, on the amount of hydrogen production rate, freshwater production rate, and system efficiency have been investigated. The results show that the energy and exergy efficiency of the proposed system is 35.75 % and 18.39 %, respectively. Moreover, the total power produced by the system is 1545 kW, the amount of hydrogen produced is 0.001175 g/s, and the freshwater production rate is 5.216 kg/s. Furthermore, the results indicated that increasing geothermal temperature and solar collector inlet volumetric flow increases hydrogen production rate. In contrast, solar irradiation and environment temperature have no effects on the hydrogen production rate of the cycle. Finally, it was found that geothermal temperature increase and collector volumetric flow show an optimum point for thermal efficiency and freshwater, respectively.

1. Introduction

In recent years, the increasing use of fossil fuels has caused many environmental problems, such as the pollution of cities, the destruction of the ozone layer, and acid rain. In addition, with the increase of industrial centers and the consumption of these fuels, the possibility of the end of fossil energy reserves has become clearer. With regard to the mentioned challenges, the

*Corresponding Author: m.abbasalizadeh@urmia.ac.ir Telephone: +98 44 31942949

doi: 10.22104/IJHFC.2022.5896.1249

use of clean and renewable energy sources such as solar energy, geothermal energy, wind energy, and waste heat energy for power production has been receiving much attention. Cogeneration systems are one of the best energy-saving methods for more efficient use of fuel to achieve environmental improvements. Cogeneration systems allow the production of electricity and useful thermal energy from a single energy source. This method is the most useful way to use primary energy because the system can simultaneously produce power, heat, and cold. Due to high energy prices and the reduction of fossil fuel resources, the optimal use of energy and its consumption management methods are critical [1-3].

The use of a new energy source, such as the completely clean fuel hydrogen, has caught the attention of researchers [4-5]. Most recently, the use of proton exchange membranes has gained much attention due to their compatibility with solar and geothermal sources and the production of purer hydrogen [6]. For example, a simple thermodynamic model for hydrogen production using a proton membrane electrolyzer system based on laboratory data was investigated by Valverde et al. [7]. Ni et al. did an analytical study as well as a comprehensive parametric study for hydrogen production using a proton membrane electrolyzer system [8]. Ahmadi et al. used ocean energy to start the organic Rankine cycle and calculated that the energy efficiency of 1 kg/22% and 2.7/3% and exergy and better hydrogen production of 6/hour are obtained [9]. In another study, Ahmadi et al. [10] proposed a new hybrid cycle based on solar energy for the simultaneous production of power, water, and hydrogen; they reported that the total cost rate is 154 dollars per hour and the exergy efficiency is 60% in the optimal state. In a survey, Ranjbar et al. [11] studied hydrogen production using a waste heat recovery system, examining the effect of important parameters. Yilmaz et al. [12] investigated seven different arrangements of geothermal and hydrogen production using the electrolyzer method and observed that the cost of hydrogen production decreases as the temperature of the geothermal source increases. Khanmohamamdi et al. [13] proposed an integrated system including a solar flat plate collector to produce electricity, cooling, and hydrogen. Their results showed that an increase in the ORC evaporator inlet temperature increases the hydrogen production rate and power generation while decreasing the cooling capacity.

Pourrahmani and Mogimi [14] investigated a trigeneration solar-driven system producing electricity, hydrogen, and cooling where the required energy for the PEM electrolyzer to produce hydrogen was provided by the gas turbine cycle. According to the results, the system produces 8.65 kg/h of hydrogen, and the exergy efficiency equals 15.28 %. Sen et al. [15] introduced a solar energy and geothermal-assisted multigeneration system to produce electricity, water, and hydrogen. Their results showed that the proposed system is capable of producing 2900 kW power, enough to produce 0.0185 kg/s of hydrogen. A multigeneration system that provides hydrogen, electricity, and hot water, including a parabolic trough collector, an organic Rankine cycle (ORC), and a PEM electrolyzer, was studied by Bozgeyik et al. [16]. The studied system can produce 20.39 kg/day of hydrogen, and the energy and exergy efficiencies are 78 % and 25.5 %, respectively. Moreover, the system's freshwater production rate was 5.74 m3/day. Hashemian and Noorpoor [17] introduced a novel geothermal-biomass-powered multi-generation plant. This system produces electricity, heating, cooling, as well as hydrogen and freshwater by applying the Rankine cycle,

a dual-effect absorption refrigeration unit, a proton exchange membrane water electrolyzer, and a biomass combustor. Their results revealed that the system could produce 31.68 MW direct power, 39.85 MW heating, 126.36 MW cooling, 23.3 m3/h freshwaters, and 88.12 kg/h hydrogen.

The literature review indicates that there is a significant interest in applying renewable energies to produce hydrogen. Therefore, the present study aims to investigate a novel multigeneration system including solar and geothermal energy sources containing a high-temperature modified Kalina cycle, an electrolyzer, a combined ORC-EJR cycle, an RO desalination unit, and a domestic water heater.

Briefly, the novelties and main goals of this study are as follows:

- Presenting a new multigeneration system applying geothermal and solar sources
- Using a modified Kalina cycle to recover solar energy
- Energy and exergy analysis of the proposed system
- Hydrogen and fresh water production from the proposed system

2. Hydrogen production processes

Various pathways for hydrogen production are shown in Figure 1. Moreover, the production methods' advantages and disadvantages, as well as their efficiency and capital cost, are presented in Table 1. It should be noted that while about 96% of worldwide hydrogen production is from fossil fuels [17], hydrogen originating from fossil fuels is low in purity and leads to the release of harmful greenhouse gases [18].

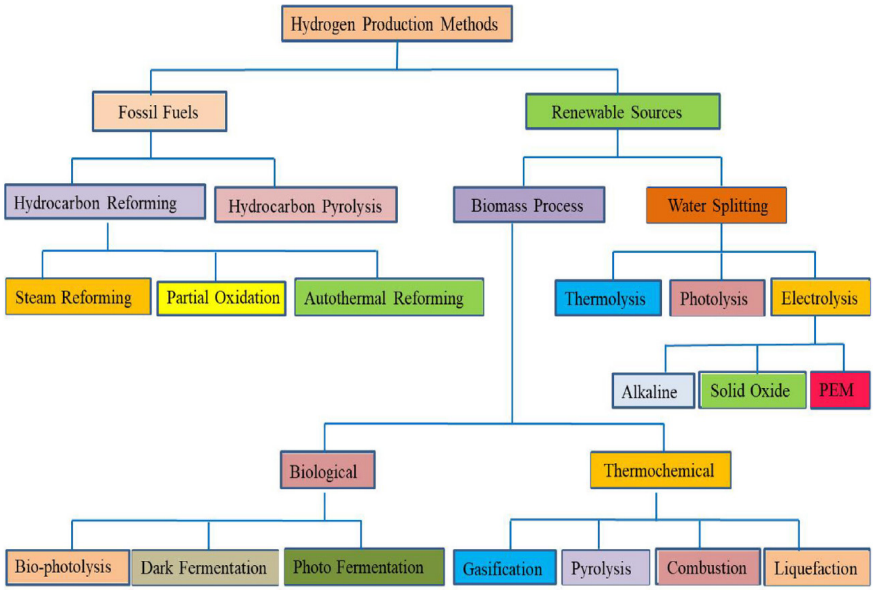

Fig. 1. Various Hydrogen Production Methods.

Table 1. Various Hydrogen production methods along with their advantages, disadvantages, efficiency, and cost [19-21].

Hydrogen production Method	Advantages	Disadvantages	Efficiency	Cost [$/kg]
Steam Reforming	Developed technology & existing infrastructure	Produced CO, CO_2 unstable supply	74–85	2.27
Auto thermal Reforming	Well-established technology & existing infrastructure	Produced CO_2 as a byproduct, use of fossil fuels	60–75	1.48
Bio photolysis	Consumes CO_2, O_2 byproduct, working under mild conditions	Low yields of H_2, sunlight needed, large reactor required, O_2 sensitivity, high cost of material	10–11	2.13
Dark Fermentation	Simple method, H_2 produced without light, no limitation O_2, CO_2-neutral, involves waste recycling	Fatty acids elimination, low yields of H_2, low efficiency, requires a huge volume of the reactor	60–80	2.57
Photo Fermentation	Involves wastewater recycling, uses different organic wastewaters, CO_2-neutral.	Low efficiency, low H_2 production rate, sunlight required, requires a huge volume of the reactor, O2-sensitivity	0.1	2.83
Gasification	Abundant, cheap feedstock and neutral CO_2	Fluctuating H_2 yields because of feedstock impurities, seasonal availability and formation of tar	30–40	1.77–2.05
Pyrolysis	Abundant, cheap feedstock and CO_2-neutral	Tar formation, fluctuating H_2 amount because of feedstock impurities and seasonal availability	35–50	1.59–1.70
Thermolysis	Clean and sustainable, O_2-byproduct, copious feedstock	High capital costs, elements toxicity, corrosion problems.	20–45	7.98–8.40
Photolysis	O_2 byproduct, abundant feedstock, no emissions	Low efficiency, non-effective photocatalytic material, requires sunlight.	0.06	8–10
Electrolysis	Established technology, zero-emission, existing Infrastructure, O_2 byproduct	Storage and transportation problems	60–80	10.30

A summary of hydrogen production by water-splitting technologies, along with their advantages, disadvantages, and efficiencies, is depicted in Table 2.

Table 2. Advantages and Disadvantages of different water electrolysis technologies [22-24].

Electrolysis process	Advantages	Disadvantages
Alkaline Electrolysis	Well-established technology, non-noble electrocatalysts, low-cost technology, energy efficiency of (70–80%), commercialized	Low current densities, formation of carbonates on the electrode, decreases the performance of the electrolyzer, low purity of gases, low operational pressure (3–30 bar) Low dynamic operation
Solid Oxide Electrolysis	Higher efficiency (90–100%), non-noble electrocatalysts, high working Pressure	Laboratory stage, large system design, low durability
Microbial Electrolysis	Uses different organic wastewaters	Under development, low hydrogen production rate, low purity of hydrogen
PEM Electrolysis	High current densities, compact system design and quick response, greater hydrogen production rate with: high purity of gases (99.99%), higher energy efficiency (80–90%), high dynamic operation	New and partially established, high cost of components, acidic environment, low durability, commercialization in near future

2.1. Principle of PEM water electrolysis

In PEM water electrolysis, water is electrochemically split into hydrogen and oxygen at their respective electrodes, such as hydrogen at the cathode and oxygen at the anode. PEM water electrolysis is accrued by pumping water to the anode, where it is split into oxygen (O_2), protons (H^+), and electrons (e^-). These protons then travel via the proton-conducting membrane to the cathode side. The electrons exit from the anode through the external power circuit, which provides the driving force (cell voltage) for the reaction. On the cathode side, the protons and electrons recombine to produce hydrogen; the following mechanism is shown in Figure 2.

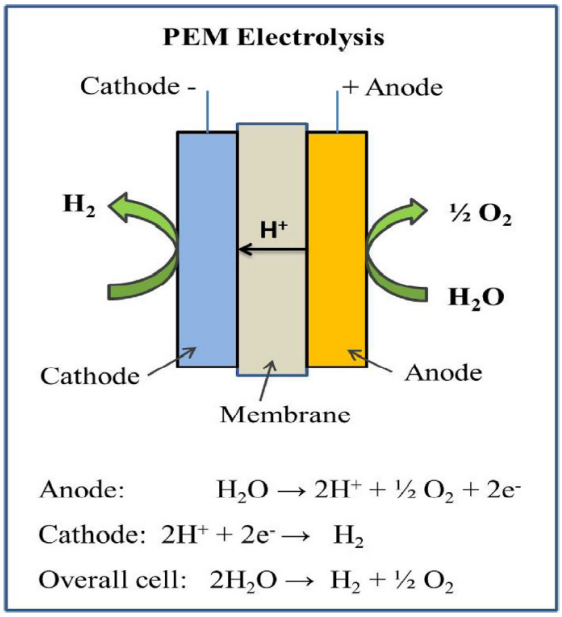

Fig. 2. Schematic of PEM water electrolysis.

3. System description

Figure 3 presents the schematic of the considered multigeneration system. As shown, the system's principal components are a low-temperature geothermal source, a solar system-based modified Kalina system, an RO desalination unit, a combined ORC-EJR cycle, a PEM electrolyzer, and a domestic water heater. The outcomes of the proposed system are electricity, fresh water, hydrogen, hot water, heating, and cooling. The primary energy sources of the system are geothermal and solar cycles. The solar cycle employed in this system has two main functions: to act as the high-temperature energy source for the Kalina cycle and to increase the temperature of the flow extracted from the ground. The parabolic trough collector absorbs energy by applying Therminol_VP1 as the base fluid. After gaining energy from the heat exchanger of the solar system, the geothermal water first enters the vapor generator of the combined ORC-EJR cycle to supply the cycle energy needed to produce power. Then, it discharges into the reinjection well, passing through the domestic water heater, which produces hot water. The generated power in the modified Kalina cycle is used as the electricity in the residential area and the source power of the RO desalination unit to purify the sea water and supply fresh water. The combined ORC-EJR cycle produces a cooling effect and power. The power generated in the combined ORC-EJR cycle is divided into two streams: employed in the residential area and applied in the PEM electrolyzer to produce hydrogen.

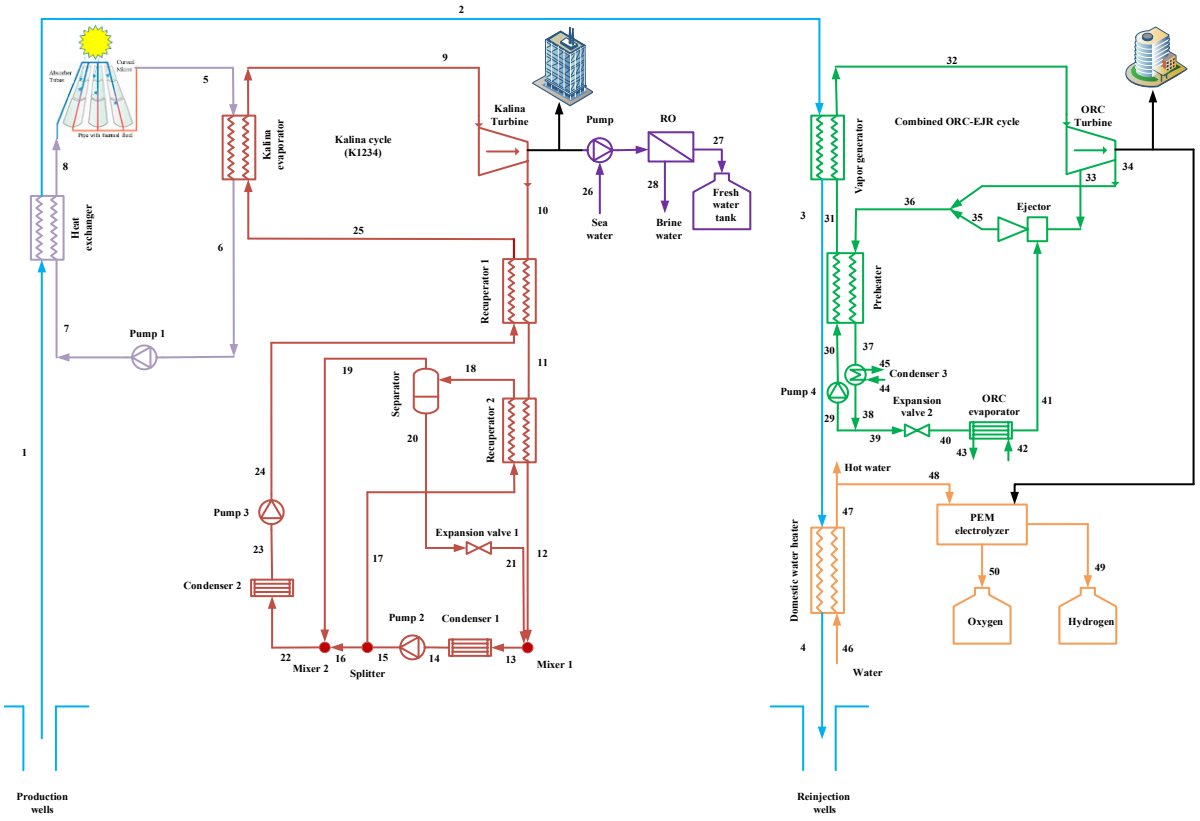

Fig. 3. Schematic diagram of the proposed multigeneration energy system.

4. Mathematical modeling

The basic equations of thermodynamics, which include mass and energy balance equations, are applied for each component of the system, and all the analyses were done by EES software [25]. To simplify the modeling, the following considerations are observed [26-27]:

- The system operates in a steady-state condition.
- There are no pressure losses in the pipes and heat exchangers.
- All turbines, pumps, condensers, and valves are assumed adiabatic systems.
- The outlet of the condensers and evaporators are considered to be saturated liquid and saturated vapor, respectively.
- Isentropic efficiency is assumed for pumps and turbines.
- Solar irradiation is presumed to be uniform and steady-state.
- Geothermal hot water is considered to be net water.

The primary input and design values of the multigeneration cycle model are exhibited in Table 3.

Table 3. The input parameters for the modeling.

Parameters	Unit	Value
GEOTHERMAL [28-29]		
Production well temperature, T_1	$(^{\circ}C)$	120
Production well Pressure, P_1	(bar)	7
SOLAR [30-32]		
Collector width, w	(m)	5.76
Collector length, L	(m)	12.27
Receiver outside diameter, $D_{o,r}$	(m)	0.07
Receiver inside diameter, $D_{i,r}$	(m)	0.066
Collector heat loss coefficient, U_L	$\left(\frac{W}{m^{2\circ}C}\right)$	3.82
Receiver inlet temperature, T_{ri}	$(^{\circ}C)$	180
The heat transfer coefficient inside the receiver, h_{fi}	$\left(\frac{W}{m^{2\circ}C}\right)$	300
The thermal conductivity of the receiver, K	$\left(\frac{W}{m^{2\circ}C}\right)$	16
Solar radiation intensity, G_b	$\left(\frac{W}{m^2}\right)$	850
Cover glazing transmissivity, τ_c	-	0.96
PTC effective transmissivity, τ_p	-	0.94
Receiver absorptivity, α_r	-	0.96
Correction factor for diffuse radiation, γ	-	0.95
KALINA [33]		
Turbine inlet ammonia concentration, x_9	-	0.49
Turbine inlet temperature, T_9	$(^{\circ}C)$	330
Turbine inlet pressure, P_9	(bar)	120
RO [34-35]		
Recovery ratio, RR	-	0.3
Number of elements, n_e	-	7
Number of pressure vessels, n_v	-	42
Seawater salinity, X_f	$\left(\frac{g}{kg}\right)$	43
ORC-EJR [38-38]		
Working fluid		Isopentane
Turbine inlet pressure, P_{32}	(bar)	6.5
Evaporator temperature, T_{40}	$(^{\circ}C)$	-5

4.1. Parabolic trough collector

The temperature of the geothermal fluid rises when it passes through Parabolic trough collectors and is calculated by the following equations [39-40]:

$$Q_u = n_{cp} n_{cs} F_R A_{ap} [S - \frac{A_r}{A_{ap}} U_L (T_{r,i} - T_0)] \quad (1)$$

S is the absorbed solar radiation and is defined as:

$$S = G_b \eta_r \quad (2)$$

$$\eta_r = \gamma \tau_c \tau_p \alpha \quad (3)$$

The following equations were used to find F_R and F_1:

$$F_R = \frac{\dot{m} c_{p,c}}{A_r U_L} [1 - \exp(-\frac{A_r U_L F_l}{\dot{m} c_{p,c}})] \quad (4)$$

$$F_1 = \frac{\frac{1}{U_L}}{\frac{1}{U_L} + \frac{D_{o,r}}{h_{fi}} + (\frac{D_{0,r}}{2k} \ln \frac{D_{o,r}}{D_{i,r}})} \quad (5)$$

The surface area of PTC is:

$$A_a = (w - D)L \quad (6)$$

4.2. Energy and exergy analysis

The main conservation equations, mass, and energy, employed in analyzing the proposed system are as follows:

$$\sum \dot{m}_{in} = \sum \dot{m}_{out} \quad (7)$$

$$\sum (\dot{m} h)_{out} - \sum (\dot{m} h)_{in} = \dot{Q} - \dot{W} \quad (8)$$

$$\dot{E} = \dot{E}_{ph} + \dot{E}_{ch} \quad (9)$$

$$\dot{E}_{ph} = \sum \dot{m}_i \left[(h_i - h_o) - T_o (s_i - s_o) \right] \quad (10)$$

$$\dot{E}_{ch} = \dot{m}_i \left[\left(\frac{x}{M_{NH3}} \right) e^o{}_{ch,NH3} + \left(\frac{1-x}{M_{H_2O}} \right) e^o{}_{ch,H_2O} \right] \quad (11)$$

In the above equations, x is the molar fraction of ammonia, and *ch* and *ph* represent the chemical, and physical exergy, respectively.

The equations used to simulate the RO unit and PEM electrolyzer are expressed in Tables 4 and 5, respectively.

Table 4. The RO unit's required modeling relations [41].

The recovery ratio	$RR = \frac{\dot{m}_{31}}{\dot{m}_{30}}$
Saline water flow rate	$\dot{m}_{32} = \dot{m}_{30} - \dot{m}_{31}$
Osmotic pressure	$P_{net} = P_{avg,f} - 75.85 \times X_{31}$
Average Osmosis pressure	$P_{avg,f} = \frac{P_{30} + P_{32}}{2} = 37.92 \times (X_{30} + X_{32})$
Temperature correction factor	$TCF = \exp\left\{2700 \times \left(\frac{1}{T+273} - \frac{1}{298}\right)\right\}$
Membrane water permeability	$K_w = \frac{6.84 \times 10^{-8} \times (18.6865 - 0.177 \times X_{32})}{(T+273)}$
High-pressure pump power	$\dot{W}_{p,RO} = \frac{\dot{m}_{30} \times \Delta P}{\rho_{30} \times \eta_p}$

Table 5. The PEM electrolyzer's required modeling relations [42].

Electrical energy consumption	$\dot{E}_{electric} = JV$
Electrolyzer voltage	$V = V_0 + V_{act,c} + V_{act,a} + V_{ohm}$
Reversible equation	$V_0 = 1.229 - 0.00085(T_{PEM} - 298)$
Activation overpotential	$A_{act,i} = \frac{RT}{F}\sinh^{-1}\left(\frac{J}{2J_{0,i}}\right) = J_a^{ref}\exp\left(\frac{-E_{act,i}}{RT}\right), i = a,c$
Ohmic overpotential	$V_{ohm} = JR_{PEM}, R_{PEM} = \int_0^L \frac{dx}{\sigma[\lambda(x)]}, \lambda(x) = \frac{\lambda_a - \lambda_c}{D}x + \lambda_c$ $\sigma[\lambda(x)] = [0.5139\lambda(x) - 0.326]\exp\left[1268\left(\frac{1}{303} - \frac{1}{T}\right)\right]$
Rate of produced H_2	$\dot{N}_{H_2,Out} = \frac{J}{2F} = \dot{N}_{H_2O,reacted}$

The transferred heat and power, as well as the exergy destruction rate of each component, can be calculated by applying the energy and exergy balance equations for the integrated system, as listed in Table 6.

Table 6. Energy conservation and exergy destruction rate relations for the system's elements.

Component	Energy balance equations	Exergy destruction rate equations
PTC field	$\dot{m}_8 h_8 + \dot{Q}_u = \dot{m}_5 h_5$	$\dot{E}x_{D,PTC} = \dot{E}x_{sun} + \dot{E}x_8 - \dot{E}x_5$
Heat exchanger	$\dot{Q}_{HX} = \dot{m}_1(h_2 - h_1) = \dot{m}_7(h_7 - h_8)$	$\dot{E}x_{D,HX} = \dot{E}x_1 + \dot{E}x_7 - \dot{E}x_2 - \dot{E}x_8$
Kalina evaporator	$\dot{Q}_{EV,KAL} = \dot{m}_5(h_5 - h_6) = \dot{m}_9(h_9 - h_{29})$	$\dot{E}x_{D,EV,KAL} = \dot{E}x_5 + \dot{E}x_{29} - \dot{E}x_6 - \dot{E}x_9$
Kalina turbine	$\dot{W}_{t,KAL} = \dot{m}_9(h_9 - h_{10})$	$\dot{E}x_{D,t,KAL} = \dot{E}x_9 - \dot{W}_{t,KAL} - \dot{E}x_{10}$
Kalina recuperator 1	$\dot{Q}_{re1,KAL} = \dot{m}_{10}(h_{10} - h_{11}) = \dot{m}_{28}(h_{29} - h_{28})$	$\dot{E}x_{D,re1,KAL} = \dot{E}x_{10} + \dot{E}x_{28} - \dot{E}x_{11} - \dot{E}x_{29}$
Kalina recuperator 2	$\dot{Q}_{re2,KAL} = \dot{m}_{11}(h_{11} - h_{12}) = \dot{m}_{18}(h_{19} - h_{18})$	$\dot{E}x_{D,re2,KAL} = \dot{E}x_{11} + \dot{E}x_{18} - \dot{E}x_{12} - \dot{E}x_{19}$
Kalina recuperator 3	$\dot{Q}_{re3,KAL} = \dot{m}_{20}(h_{20} - h_{21}) = \dot{m}_{27}(h_{28} - h_{27})$	$\dot{E}x_{D,re3,KAL} = \dot{E}x_{20} + \dot{E}x_{27} - \dot{E}x_{21} - \dot{E}x_{28}$
Kalina recuperator 4	$\dot{Q}_{re4,KAL} = \dot{m}_{17}(h_{17} - h_{18}) = \dot{m}_{22}(h_{23} - h_{22})$	$\dot{E}x_{D,re4,KAL} = \dot{E}x_{17} + \dot{E}x_{22} - \dot{E}x_{18} - \dot{E}x_{23}$
Kalina mixer 1	$\dot{m}_{12} h_{12} + \dot{m}_{24} h_{24} = \dot{m}_{13} h_{13}$	$\dot{E}x_{D,mx1,KAL} = \dot{E}x_{12} + \dot{E}x_{24} - \dot{E}x_{13}$
Kalina mixer 2	$\dot{m}_{16} h_{16} + \dot{m}_{21} h_{21} = \dot{m}_{25} h_{25}$	$\dot{E}x_{D,mx2,KAL} = \dot{E}x_{16} + \dot{E}x_{21} - \dot{E}x_{25}$
Kalina condenser 1	$\dot{Q}_{con1,KAL} = \dot{m}_{13}(h_{13} - h_{14})$	$\dot{E}x_{D,con1,KAL} = \dot{E}x_{13} - \dot{E}x_{14} - \dot{Q}_{con1,KAL}\left(1 - \frac{T_0}{T_{14}}\right)$
Kalina condenser 2	$\dot{Q}_{con2,KAL} = \dot{m}_{25}(h_{25} - h_{26})$	$\dot{E}x_{D,con2,KAL} = \dot{E}x_{25} - \dot{E}x_{26} - \dot{Q}_{con2,KAL}\left(1 - \frac{T_0}{T_{26}}\right)$
Kalina pump 2	$\dot{W}_{p2,KAL} = \dot{m}_{14}(h_{15} - h_{14})$	$\dot{E}x_{D,p2,KAL} = \dot{W}_{p2,KAL} + \dot{E}x_{14} - \dot{E}x_{15}$
Kalina pump 3	$\dot{W}_{p3,KAL} = \dot{m}_{26}(h_{27} - h_{26})$	$\dot{E}x_{D,p3,KAL} = \dot{W}_{p3,KAL} + \dot{E}x_{26} - \dot{E}x_{27}$
Kalina splitter	$\dot{m}_{15} h_{15} = \dot{m}_{16} h_{16} + \dot{m}_{17} h_{17}$	$\dot{E}x_{D,spl,KAL} = \dot{E}x_{15} - \dot{E}x_{16} - \dot{E}x_{17}$
Kalina separator	$\dot{m}_{19} h_{19} = \dot{m}_{20} h_{20} + \dot{m}_{22} h_{22}$	$\dot{E}x_{D,sep,KAL} = \dot{E}x_{19} - \dot{E}x_{20} - \dot{E}x_{22}$
Kalina expansion valve 1	$h_{23} = h_{24}$	$\dot{E}x_{D,exv1,KAL} = \dot{E}x_{23} - \dot{E}x_{24}$
ORC vapor generator	$\dot{Q}_{vg,ORC-ERC} = \dot{m}_2(h_2 - h_3) = \dot{m}_{35}(h_{36} - h_{35})$	$\dot{E}x_{D,vg,ORC-ERC} = \dot{E}x_2 + \dot{E}x_{35} - \dot{E}x_3 - \dot{E}x_{36}$
ORC turbine	$\dot{W}_{t,ORC-ERC} = \dot{m}_{36}(h_{36} - h_{37}) + \dot{m}_{38}(h_{37} - h_{38})$	$\dot{E}x_{D,t,ORC-ERC} = \dot{E}x_{36} - \dot{W}_{t,ORC-ERC} - \dot{E}x_{37} - \dot{E}x_{38}$
ORC ejector	$\mu_{eje} = \frac{\dot{m}_{45}}{\dot{m}_{37}}$	$\dot{E}x_{D,eje,ORC-ERC} = \dot{E}x_{37} + \dot{E}x_{45} - \dot{E}x_{39}$
ORC preheater	$\dot{Q}_{ph,ORC-ERC} = \dot{m}_{34}(h_{35} - h_{34}) = \dot{m}_{40}(h_{40} - h_{41})$	$\dot{E}x_{D,ph,ORC-ERC} = \dot{E}x_{34} + \dot{E}x_{40} - \dot{E}x_{35} - \dot{E}x_{41}$
ORC pump 4	$\dot{W}_{p,ORC-ERC} = \dot{m}_{33}(h_{34} - h_{33})$	$\dot{E}x_{D,p4,ORC-ERC} = \dot{W}_{p4,ORC-ERC} - \dot{E}x_{33} + \dot{E}x_{34}$
ORC condenser 3	$\dot{Q}_{con3,ORC-ERC} = \dot{m}_{41}(h_{41} - h_{42}) = \dot{m}_{48}(h_{49} - h_{48})$	$\dot{E}x_{D,con3,ORC-ERC} = \dot{E}x_{41} + \dot{E}x_{48} - \dot{E}x_{42} - \dot{E}x_{49}$
ORC expansion valve 2	$h_{43} = h_{44}$	$\dot{E}x_{D,exv2,ORC-ERC} = \dot{E}x_{43} - \dot{E}x_{44}$
ORC evaporator	$\dot{Q}_{eva,ORC-ERC} = \dot{m}_{44}(h_{45} - h_{44})$	$\dot{E}x_{D,EV,ORC-ERC} = \dot{E}x_{44} + \dot{E}x_{46} - \dot{E}x_{45} - \dot{E}x_{47}$
PEM	$\dot{W}_{PEM} = (\dot{m}_{52} h_{52} - \dot{m}_{53} h_{53} - \dot{m}_{54} h_{54})$	$\dot{E}x_{D,PEM} = \dot{E}x_{52} + \dot{W}_{PEM} - \dot{E}x_{53} - \dot{E}x_{54}$
DWH	$\dot{Q}_{DWH} = \dot{m}_3(h_3 - h_4) = \dot{m}_{50}(h_{51} - h_{50})$	$\dot{E}x_{DWH} = \dot{E}x_3 + \dot{E}x_{50} - \dot{E}x_4 - \dot{E}x_{51}$
RO	$\dot{W}_{RO} = (\dot{m}_{30} h_{30} - \dot{m}_{31} h_{31} - \dot{m}_{32} h_{32})$	$\dot{E}x_{D,RO} = \dot{E}x_{30} - \dot{E}x_{31} - \dot{E}x_{32}$

Finally, the overall energy and exergy efficiency of the proposed multigeneration system can be calculated with the following equations:

(12)

$$\eta_{th,tot} = \frac{\dot{W}_{KAL} + \dot{W}_{ORC-ERC} + \dot{Q}_{cooling} + \dot{Q}_{DWH} + \dot{m}_{53} HHV_{H2} - \dot{W}_{PEM} + \dot{m}_{31} h_{31} - \dot{W}_{RO}}{\dot{Q}_u + \dot{m}_1 h_1}$$

(13)

$$\eta_{ex,tot} = \frac{\dot{W}_{KAL} + \dot{W}_{ORC-ERC} + \dot{E}x_{cooling} + \dot{E}x_{53} + \dot{E}x_{54} + \dot{E}x_{51} - \dot{E}x_{50} + \dot{E}x_{31}}{\dot{E}x_{in,sun} + \dot{E}x_1}$$

5. Validation

As the proposed system is a novel multigeneration system, some of the system's main elements have been validated with previous studies to define the precision of the simulation. The results of the RO desalination unit have been compared with the results of Nafey and Sharaf [43] in Table 7. Based on the comparison, an appropriate agreement can be seen between the present simulation and previous studies.

Table 7. Validation of the modeling results for the RO desalination unit.

Variable	Unit	Present study	[Nafey and Sharaf [43
SPC	kWh/m^3	7.733	7.68
$\dot{W}_{pump,RO}$	kW	1127	1131
M_f	$\frac{m^3}{h}$	485.8	485.9
M_b	$\frac{m^3}{h}$	340	340.1
X_b	-	0.06418	0.06418
X_d	-	0.000252	0.00025
SR	-	0.9944	0.9944
ΔP	kPa	6871	6850

6. Results and discussion

A geothermal source combined with a high-temperature PTC was used in this study to generate several productions containing power, cooling, domestic water heating hydrogen, and desalination. EES software was used to model the geothermal-solar multigeneration system. Parametric analysis was performed to study the effects of varying several critical parameters (solar irradiation, environmental and geothermal temperature, solar collector inlet temperature, and volumetric flow) on the production of the proposed system. Mostly, the results are for the hydrogen generation rate. Freshwater production rate and efficiencies.

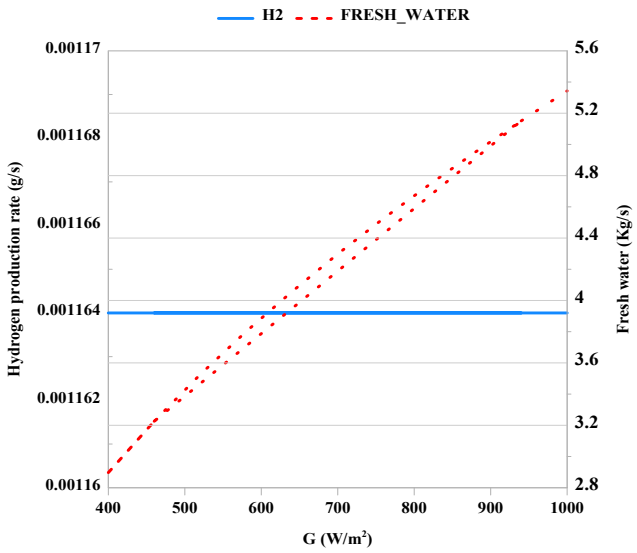

Fig. 4. Effect of solar irradiation on the hydrogen and freshwater production rates.

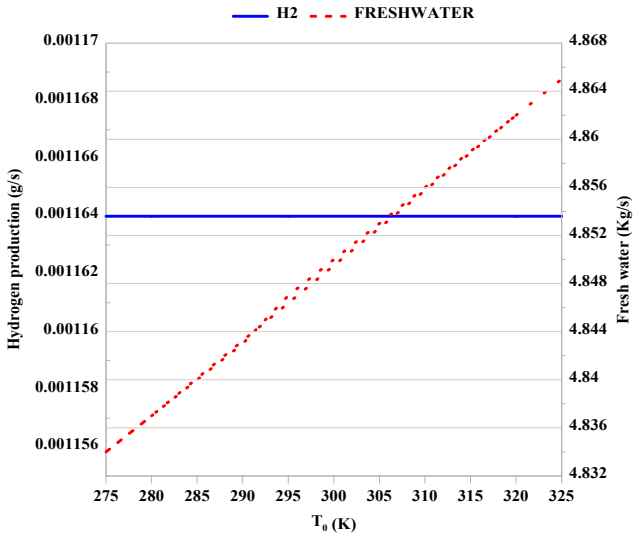

Fig. 5. Effect of different environmental temperatures on the hydrogen and freshwater production rates.

The effect of increasing solar irradiation on the produced hydrogen rate and freshwater production rate is shown in Figure 4. The diagram shows that as solar irradiation rises, the production of freshwater increases, while hydrogen production is fixed without any change. Paying attention to the schematic diagram of the cycle makes it clear that the Kalina cycle is responsible for freshwater generation, and the ORC cycle produces hydrogen. Changes in solar irradiation affect the Kalina cycle but do not affect the ORC cycle. Therefore, the graphs are increasing for freshwater and fixed for hydrogen production rates.

Figure 5 shows the effect of environmental temperature differences on the hydrogen production and freshwater production rates and indicates that as the environmental temperature increases, the value of the Kalina cycle power production increases, but the value of the ORC power production remains unchanged. This process increases the freshwater production rate and fixes the hydrogen production rate.

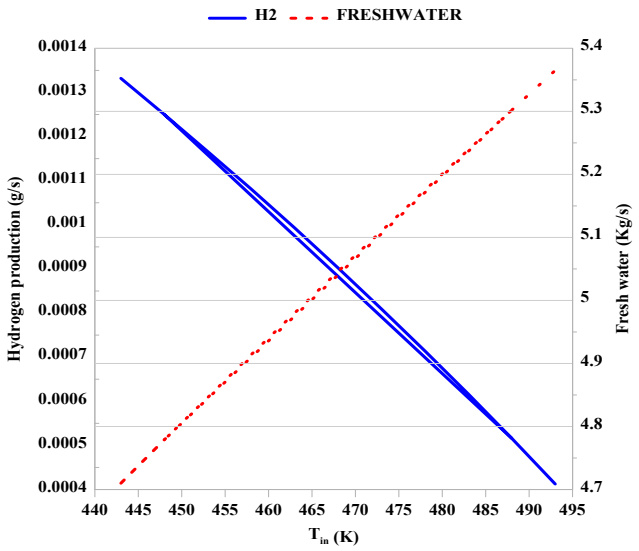

Fig.6. Effect of solar collector inlet temperature on the hydrogen and freshwater production rates.

Figure 6 depicts the variation in the hydrogen and freshwater production rates with changes in the solar collector's inlet temperature. According to the graphs, when the inlet temperature increases from 443 to 493 K, the freshwater production rate increases from 4.71 to 5.36 while the hydrogen production rate decreases from 0.00134 to 0.00041. As the solar collector inlet temperature increases, the Kalina cycle power output increases, and the ORC cycle power output decreases.

The effect of increasing geothermal temperature on hydrogen production and freshwater can be seen schematically in Figure 7. As the geothermal temperature increases, the amount of energy input to the Organic Rankine cycle increases, causing the power of the Rankine cycle turbine to rise, and, in this case, hydrogen production will increase. Moreover, Kalina cycle net power production is irrelevant to the geothermal temperature change.

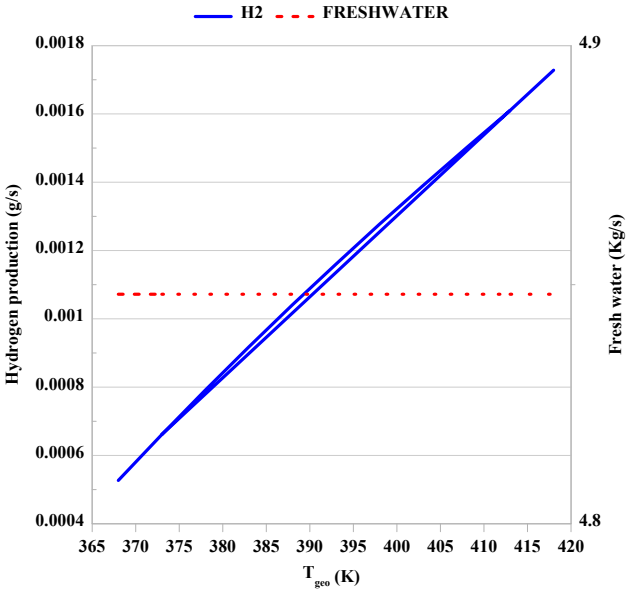

Fig. 7. Effect of geothermal temperature on hydrogen and freshwater production rates.

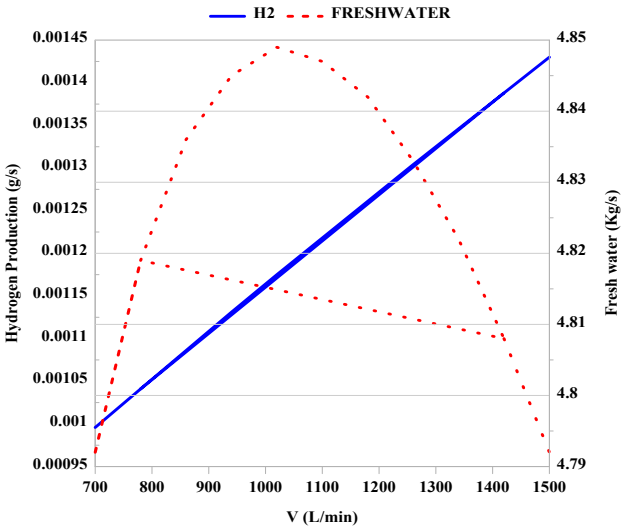

Fig. 8. Effect of volumetric flow on hydrogen and freshwater production rates.

Figure 8 shows the effect of the collector volumetric flow on the hydrogen and freshwater generation rates. The graphs show that when the volumetric flow changes from 700 to 1500 L/min, the amount of the hydrogen production rate increases from 0.001 to 0.00143 g/s, but fresh water production rate first increases from 4.79 to 4.85 kg/s and then decreases to 4.79 kg/s, the turning point happens at 1020 L/min.

Figure 9 indicates how changes in solar irradiation affect variations in the total efficiencies and power produced by the system. According to the results, when solar irradiation rises, the energy and exergy efficiencies decrease, and produced power increases. Increasing the solar irradiance increase the total amount of the energy input to the Kalina cycle and causes an increase in the net power output of the system. On the other hand, increasing solar irradiation leads to an increase in the useful amount of energy obtained from the solar cycle. Therefore, according to energy and exergy relations, the energetic and exergetic efficiencies will decrease.

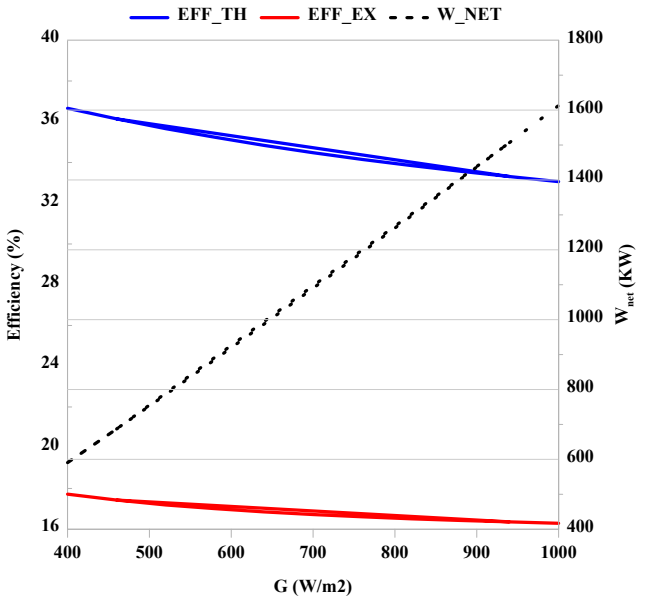

Fig. 9. Effect of solar irradiation on the total efficiency and net power.

The effect of the changes in the thermal and exergy efficiency of the system is shown in Figure 10. The ex-

ergetic efficiency varies from 14.91 to 17.84 % when the geothermal temperature rises from 368 to 418 K. Conversely, the thermal efficiency first decreases from 34.75 to 33.7 %, and then around 390 K starts rising to 34.42 %.

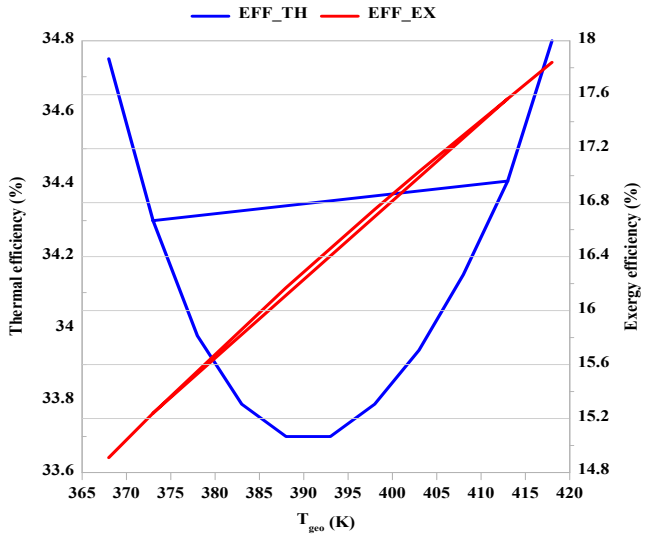

Fig. 10. Effect of geothermal temperature on thermal and exergy efficiency of the system.

7. Conclusions

Nowadays, the use of clean energy and alternative fuel is widespread. In this review, a new cycle has been introduced based on geothermal and solar energies. The multigeneration system produces hydrogen using the proton membrane electrolyzer process from the ORC cycle and fresh water from the Kalina cycle, in addition to power, cooling, and heating. In this research, the effects of parameters affecting hydrogen and freshwater production have been investigated, and the results are summarized as follows:

- In the initial investigation of the proposed cycle, the net power is 1545 kW, the hydrogen production rate is 0.001175 g/s, the freshwater production rate is 5.216 kg/s, and energy and exergy efficiencies are 35.75, and 18.39 %, respectively.
- Increasing solar irradiation increases freshwater and net power production, decreases thermal and exergy efficiency, while the amount of hydrogen production remains constant.
- The amount of hydrogen produced by increasing the environmental temperature remains constant, but freshwater production increases.
- Increasing solar collector inlet temperature decreases the hydrogen produced while the freshwater rate increases.
- An increase in geothermal temperature causes an increase in hydrogen production rate and exergy efficiency while the amount of freshwater produced is fixed.
- Increasing the solar collector volumetric flow increases the hydrogen production rate while the freshwater production value is optimum.

References

[1]Dincer I., »Renewable energy and sustainable development: a crucial review«, Renewable and Sustainable Energy Reviews, 2000, 4:157.

[2]Ghaebi H, Amidpour M, Karimkashi S, Rezayan O, “Energy, exergy and thermoeconomic analysis of a combined cooling, heating and power (CCHP) system with gas turbine prime mover”, International Journal of Energy Research, 2011, 35:697.

[3]Dincer I. and Rosen M.A., Exergy: energy, environment and sustainable development, Newnes, 2012.

[4]Ozgur T and Yakaryılmaz AC., “A review: Exergy

analysis of PEM and PEM fuel cell-based CHP systems", International Journal of Hydrogen Energy, 2018, 43:17993.

[5]Orhan MF and Babu BS., "Investigation of an integrated hydrogen production system based on nuclear and renewable energy sources: Comparative evaluation of hydrogen production options with a regenerative fuel cell system", Energy, 2015, 88:801.

[6]Pham AT, Baba T and Shudo T., "Efficient hydrogen production from aqueous methanol in a PEM electrolyzer with porous metal flow field: Influence of change in grain diameter and material of porous metal flow field", International Journal of Hydrogen Energy, 2013, 38:9945.

[7]Garcia-Valverde R, Espinosa N and Urbina A., "Simple PEM water electrolyzer model and experimental validation", International Journal of Hydrogen Energy, 2012, 37:1927.

[8]Ni M, Leung MKH and Leung DYC., "Energy and exergy analysis of hydrogen production by a proton exchange membrane (PEM) electrolyzer plant", Energy Conversion and Management, 2008, 49:2748.

[9]Ahmadi P, Dincer I and Rosen MA., "Energy and exergy analyses of hydrogen production via solar-boosted ocean thermal energy conversion and PEM electrolysis", International Journal of Hydrogen Energy, 2013, 38:1795.

[10]Ahmadi P, Dincer I and Rosen MA., "Multi-objective optimization of a novel solar-based multigeneration energy system", Solar Energy, 2014, 108:576.

[11]Ranjbar SF, Nami H, Khorshid A and Mohammadpour, H, "Hydrogen production using waste heat recovery of MATIANT non-emission system via PEM electrolysis.", Modares Mechanical Engineering, 2016, 16:42.

[12]Yilmaz C, Kanoglu M, Bolatturk A and Gadalla M., "Economics of hydrogen production and liquefaction by geothermal energy", International Journal of Hydrogen Energy, 2012, 37:2058-2069.

[13]Khanmohammadi S, Heidarnejad P, Javani N and Ganjehsarabi HA., "Exergoeconomic analysis and multi objective optimization of a solar based integrated energy system for hydrogen production", International Journal of Hydrogen Energy, 2017, 42:21443.

[14]Pourrahmani H and Moghimi M., "Exergoeconomic analysis and multi-objective optimization of a novel continuous solar-driven hydrogen production system assisted by phase change material thermal storage system", Energy, 2019, 15;189:116170.

[15]Sen O, Guler OF, Yilmaz C and Kanoglu M., "Thermodynamic modeling and analysis of a solar and geothermal assisted multi-generation energy system", Energy Conversion and Management, 2021, 239:114186.

[16]Bozgeyik A, Altay L and Hepbasli A., "A parametric study of a renewable energy based multigeneration system using PEM for hydrogen production with and without once-through MSF desalination", International Journal of Hydrogen Energy, 2022, 47:31742.

[17]Boreum L, Juheon H, Sehwa K, Choonghyun S, Changhwan M, Sangbong M and Hankwon L., "Economic feasibility studies of high-pressure PEM water electrolysis for distributed H2 refu-

eling stations", Energy Conversion and Management, 2018, 162:139.

[18]Holladay JD, Hu J, King DL, and Wang Y., "An overview of hydrogen production technologies", Catalysis today, 2009, 139:244.

[19]Chi J. and Yu H., "Water electrolysis based on renewable energy for hydrogen production", Chinese Journal of Catalysis, 2018, 39:390.

[20]Rand, DA., "A journey on the electrochemical road to sustainability", Journal of Solid-State Electrochemistry", 2011, 15:1579.

[21]Züttel A., "Hydrogen storage methods", Naturwissenschaften, 2004, 91:157.

[22]Kumar SS and Himabindu V., "Hydrogen production by PEM water electrolysis–A review", Materials Science for Energy Technologies, 2019, 2:442.

[23]Kamaroddin MFA, Sabli N, Nia PM, Abdullah TAT, Abdullah LC, Izhar S, Ripin A and Ahmad A., "Phosphoric acid doped composite proton exchange membrane for hydrogen production in medium-temperature copper chloride electrolysis", International Journal of Hydrogen Energy, 2020, 45:22209.

[24]Bessarabov D, Wang H, Li H and Zhao N., "PEM electrolysis for hydrogen production: principles and applications", CRC press, 2016.

[25]Hashemian N and Noorpoor A., "A geothermal-biomass powered multi-generation plant with freshwater and hydrogen generation options: Thermo-economic-environmental appraisals and multi-criteria optimization", Renewable Energy, 2022, 198:254.

[26]EES. Engineering equation solver, 2018.

[27]Kianfard H., Khalilarya S. and Jafarmadar S., "Exergy and exergoeconomic evaluation of hydrogen and distilled water production via combination of PEM electrolyzer, RO desalination unit and geothermal driven dual fluid ORC", Energy conversion and management, 2018, 177:339.

[28]Musharavati F., Khanmohammadi S. and Pakseresht A, "A novel multi-generation energy system based on geothermal energy source: Thermo-economic evaluation and optimization", Energy Conversion and Management, 2021, 230:113829.

[29]Alirahmi S.M., Rostami M. and Farajollahi A.H., "Multi-criteria design optimization and thermodynamic analysis of a novel multi-generation energy system for hydrogen, cooling, heating, power, and freshwater", International Journal of Hydrogen Energy, 2020, 45:15047.

[30]Al-Hamed K.H.M. and Dincer I., "Investigation of a concentrated solar-geothermal integrated system with a combined ejector-absorption refrigeration cycle for a small community", International Journal of Refrigeration, 2019, 106:407.

[31]Al-Sulaiman F.A., "Exergy analysis of parabolic trough solar collectors integrated with combined steam and organic Rankine cycles", Energy Conversion and Management, 2013, 77:441.

[32]Alirahmi S.M., Rahmani Dabbagh S., Ahmadi, P. and Wongwises, S., "Multi-objective design optimization of a multi-generation energy system based on geothermal and solar energy", Energy Conversion and Management, 2020, 205:112426.

[33]Yüksel, Y.E., "Thermodynamic assessment of

modified Organic Rankine Cycle integrated with parabolic trough collector for hydrogen production", International Journal of Hydrogen Energy, 2018, 43:5832.

[34]Sarabchi N., Mahmoudi S.S., Yari M. and Farzi, A., "Exergoeconomic analysis and optimization of a novel hybrid cogeneration system: High-temperature proton exchange membrane fuel cell/Kalina cycle, driven by solar energy", Energy Conversion and Management, 2019, 190:14.

[35]Nafey A.S and Sharaf M.A., "Combined solar organic Rankine cycle with reverse osmosis desalination process: energy, exergy, and cost evaluations", Renewable Energy, 2010, 35:2571.

[36]Nemati, A., Sadeghi, M. and Yari, M, "Exergoeconomic analysis and multi-objective optimization of a marine engine waste heat driven RO desalination system integrated with an organic Rankine cycle using zeotropic working fluid", Desalination, 2017, 422:113.

[37] Habibzadeh A, Rashidi M.M. and Galanis N., "Analysis of a combined power and ejector-refrigeration cycle using low temperature heat", Energy Conversion and Management, 2013, 65:381.

[38]Aliahmadi M., Moosavi A. and Sadrhosseini H., "Multi-objective optimization of regenerative ORC system integrated with thermoelectric generators for low-temperature waste heat recovery", Energy Reports, 2021, 7:300.

[39]Takleh H.R. and Zare, V., "Proposal and thermoeconomic evaluation with reliability considerations of geothermal driven trigeneration systems with independent operations for summer and winter", International Journal of Refrigeration, 2021, 127:34.

[40]Kalogirou S.A., Solar energy engineering: processes and systems. Academic Press, 2013.

[41]Yüksel Y.E., "Thermodynamic assessment of modified Organic Rankine Cycle integrated with parabolic trough collector for hydrogen production", International Journal of Hydrogen Energy, 2018, 43:5832.

[42]Nafey A.S. and Sharaf M.A., "Combined solar organic Rankine cycle with reverse osmosis desalination process: energy, exergy, and cost evaluations", Renewable Energy, 2010, 35:2571.

[43]Abdolalipouradl M, Khalilarya S and Jafarmadar S., "Energy and exergy analysis of a new power, heating, oxygen and hydrogen cogeneration cycle based on the Sabalan Geothermal Wells", International Journal of Engineering, 2019, 32:445.